Cancer Chemother Pharmacol (2003) 51: 337–348
DOI 10.1007/s00280-003-0571-6

ORIGINAL ARTICLE

**Philip C. Mack · David R. Gandara
Alvin H. Lau · Primo N. Lara Jr.
Martin J. Edelman · Paul H. Gumerlock**

Cell cycle-dependent potentiation of cisplatin by UCN-01 in non-small-cell lung carcinoma

Received: 25 June 2002 / Accepted: 13 December 2002 / Published online: 25 March 2003

Abstract *Purpose*: We evaluated the combination of UCN-01 plus cisplatin and sought to determine how the cell cycle effects of each agent affected the combined response. Cisplatin-induced DNA damage results in cell cycle arrest, primarily at the S and G_2 checkpoints, providing the opportunity for DNA damage repair prior to mitosis. Thus, strategies to enhance cisplatin cytotoxicity include attenuation of DNA damage-induced checkpoints. The cyclin-dependent kinase inhibitor 7-hydroxystaurosporine (UCN-01) can potentiate cisplatin activity, likely via abrogation of the S and G_2 checkpoints. UCN-01 has additional effects on cell cycling, including induction of an *RB*-associated G_1 arrest. *Methods*: NSCLC cell lines A549 (wt *p53*, wt *RB*), Calu1 (*p53*-null, wt *RB*) and H596 (mt *p53*, *RB*-null) were treated with UCN-01 and/or cisplatin with two-drug treatments delivered in alternate sequences. Effects of drug treatment on cell growth, cell cycling, apoptosis and levels and phosphorylation of cell cycle-associated proteins were evaluated. The interaction between the two drugs was assessed using median effect analysis. *Results*: When UCN-01 preceded cisplatin, growth inhibition was additive or less than additive, as assessed by median effect analysis. In contrast, when NSCLC cells were treated with cisplatin followed by UCN-01, the combination was synergistic. In this treatment sequence, a decrease in the proportion of cells at the G_2 checkpoint was confirmed by reduced expression of cyclins A and B and activation of Cdk1. Abrogation of the G_2 DNA damage checkpoint and apoptosis were prevalent only in cell populations treated with cisplatin followed by UCN-01 and was markedly enhanced in the cell lines with disrupted *p53*. *Conclusions*: These studies indicate that timing of drug administration strongly influences response to cisplatin plus UCN-01 in NSCLC cells, and this is related to the cell cycle-modulatory effects of these agents. Furthermore, this sequence combination was more effective in cell lines with dysfunctional *p53*. These findings support the hypothesis that checkpoint abrogation is the major mechanism of UCN-01-mediated potentiation of cisplatin cytotoxicity.

Keywords 7-Hydroxystaurosporine · UCN-01 · NSCLC · Checkpoint abrogation · p53

This study was supported in part by grants from the National Institutes of Health (CA62505 and CA63265), the Veterans Administration (M.J.E.), the University of California President's Undergraduate Fellowship (A.H.L.), and the American Cancer Society (ACS-CRTG-0019701CCE to P.N.L. and ACS-CA 4-8-99 to P.C.M.).

P. C. Mack · D. R. Gandara · A. H. Lau · P. N. Lara Jr.
P. H. Gumerlock (✉)
Cancer and Molecular Research Laboratory,
Division of Hematology/Oncology,
Department of Internal Medicine,
University of California, Davis Cancer Center, 4501 X Street,
Sacramento, CA 95817, USA
E-mail: paul.gumerlock@ucdmc.ucdavis.edu
Tel.: +1-916-7348614
Fax: +1-916-7342361

M. J. Edelman · D. R. Gandara
Northern California Veterans Administration Systems of Clinics,
Martinez, CA, USA

Present address: M. J. Edelman
University of Maryland, Baltimore, MD, USA

Introduction

Until recently, few chemotherapeutic agents have demonstrated reproducible activity against non-small-cell lung cancer (NSCLC), which accounts for approximately 80% of all lung cancer cases. In an analysis of over 2000 patients with advanced NSCLC treated on clinical trials of the Southwest Oncology Group (SWOG), therapy based on cisplatin (CDDP) emerged as an independent prognostic variable predicting improved survival [6, 18]. Platinum-based therapy remains the standard for treatment of locally advanced (stage III) and metastatic (stage IV) disease.

CDDP exerts its antitumor effects via the formation of DNA adducts and crosslinks, resulting in S-phase delay and G_2 arrest [16]. Arrest at the G_2 checkpoint is a

protective mechanism that allows cells to repair DNA damage before entering mitosis [1, 12, 40]. Consistent with this, resistance to CDDP has been associated with increased nucleotide excision repair capabilities [17]. Compounds that shorten or abrogate the G_2 checkpoint, including methylxanthines (e.g., caffeine), phosphatase inhibitors (e.g., okadaic acid) and kinase inhibitors (e.g., staurosporine) have been reported to potentiate cytotoxicity of DNA-damaging agents in vitro [17, 33, 34, 57]. Because these agents have demonstrated little clinical utility, novel drugs that can effectively abrogate the G_2 checkpoint in a clinical setting are of considerable interest since they may limit repair of chemotherapy-induced DNA damage and thereby increase the therapeutic index. One such agent currently under investigation is 7-hydroxystaurosporine (UCN-01), a kinase inhibitor derived from *Streptomyces* [47, 48, 52]. UCN-01 has been shown to cause G_1 arrest and abrogation of DNA-damage-induced checkpoint arrests [4, 5, 8, 9, 34, 35, 49, 56]. Additionally, it inhibits protein kinase C (PKC), modulates activity of cyclin-dependent kinases (Cdks) and induces expression of Cdk inhibitors [2, 5, 32, 35, 44, 52, 55]. Potentiation of the anticancer activities of radiation, CDDP, mitomycin C, camptothecin and other DNA-damaging agents by UCN-01 has been reported [3, 8, 31, 38, 51, 54, 56]. UCN-01 appears to potentiate DNA-damaging agents by reducing the period of S and/or G_2 arrest (checkpoint abrogation), limiting repair of DNA, an effect that has been found to be greater in cells with disrupted *p53* [3, 31, 38, 51, 56].

The DNA-damage-induced G_2 phase checkpoint is primarily regulated by the complex formed by Cyclin B and Cdk1, which directs progression of cells into M phase [7, 39, 45]. Activation of Cdk1 requires a number of steps in addition to cyclin B binding: the complex must be located in the nucleus, be activated by phosphorylation at Thr161, be free of Cdk inhibitors such as $p21^{CDKN1}$, and be free of inhibitory phosphorylation at Thr14 and Tyr15 [19, 20, 42]. In response to DNA damage, the phosphatase Cdc25C, which normally serves to remove Cdk1 inhibitory phosphorylation, is itself inactivated by Chk1 or Chk2 via phosphorylation on Ser216 [22, 41, 43, 46]. Studies with UCN-01 in vitro have demonstrated potent inhibition of Chk1-mediated phosphorylation of Cdc25C [11, 25, 45]. Thus, after DNA damage, inhibition of Chk1 by UCN-01 promotes premature activation of Cdk1 and exit from G_2 arrest. In addition, since *p53* has an independent role in the maintenance of G_2 arrest following DNA damage, lack of function of this tumor suppressor due to mutation or deletion also contributes to the exit from G_2 [10, 34, 53].

Since UCN-01 and CDDP have effects at multiple points in the cell cycle, we hypothesized that the efficacy of combination treatment would be dependent on the timing of the two-drug administration. Further, it was expected that the status of *p53* (a gene commonly disrupted in NSCLC) would also influence response. To test this, we investigated the combination of CDDP plus UCN-01 with regard to sequence-specificity, apoptosis and cell cycle-related effects in NSCLC cell lines with different *p53* status: wild-type (wt), mutant (mt), or null.

Materials and methods

Cell cultures

The NSCLC cell lines A549, Calu1 and H596 were acquired from the American Type Culture Collection (Rockville, Md.). Cells were maintained under standard conditions as previously reported [35].

Drug treatment

Stock solutions were prepared by dissolving UCN-01 in DMSO at a concentration of 1 mg/ml and were stored at −40°C. Immediately prior to treatment, the UCN-01 stock solution was further diluted in serum-free medium. UCN-01 was kindly provided by the Drug Synthesis and Chemistry Branch, Developmental Therapeutics Program, Division of Cancer Treatment, National Cancer Institute. Stock solutions of CDDP were formulated in a 150 m*M* NaCl solution at a concentration of 1 mg/ml and used fresh.

p53 functional assay

The yeast functional assay of *p53* alleles was performed on A549 and H596 cell lines following the method of Flaman et al. [15, 21]. The yeast strain yIG397, which contains an integrated plasmid with the *ADE2* gene under the control of a p53-responsive promoter and the plasmids pLS76 and pRDI-22, were graciously provided by Dr. Richard Iggo (Oncogene Group, Swiss Institute for Experimental Cancer Research, Epalinges, Switzerland). The plasmid pRDI-22 was digested using *Hin*DIII and *Stu*I to create a gap between codons 67 and 347 of the wt *p53* insert. The cell line *p53* RT-PCR products spanning codons 53 through 364 and the gapped pRDI-22 were cotransfected into the yIG397 yeast using the lithium acetate polyethylene glycol-3350 (LiOAc-PEG) method of yeast transfection. The transfected yeast cells were grown at 35°C for 3 days on dishes containing synthetic minimal medium lacking leucine, supplemented with 5 μg/ml of adenine, and then stored at 4°C for 2–4 days to enhance color development. Transactivational function of the specific *p53* allele is scored based on the color of yeast colonies. Large white colonies indicate wt transactivational function; small red colonies, resulting from limited growth and the accumulation of intermediate products in adenine metabolism, are scored as total loss of function. More than 200 yeast colonies were counted for each transfection in two separate experiments per cell line.

Western blotting

Protein extraction, gel electrophoresis and Western blotting were performed as previously reported [35]. Briefly, soluble proteins were extracted and the lysate was cleared by centrifugation. Protein concentrations were quantitated from duplicate readings using a modified Bradford assay (Bio-Rad Laboratories, Richmond, Calif.). Protein samples were diluted with lysis buffer to either 20 or 30 μg/μl to facilitate equal loading of samples. SDS-PAGE gels were cast using a discontinuous gel system as previously reported [35]. Cdk1, $p27^{KIP1}$, $p21^{CDKN1}$ and β-actin were separated on 15% gels and Cyclins A and B were separated on 10% gels using a minigel system (Protean II, Bio-Rad Laboratories). Proteins were transferred to nitrocellulose membranes (Bio-Rad Laboratories) at a constant 125 V for 80 min or at 40 V overnight. After blocking with a 4% powdered milk solution in TBST (25 m*M* Tris-HCl (pH 8.0), 125 m*M* NaCl, 0.1% Tween 20), blots were incubated either overnight at 4°C or at room temperature for 1 h with one of the following primary antibodies: p27 rabbit polyclonal, Cyclin B1

mouse monoclonal and Cyclin A rabbit polyclonal (Santa Cruz Biotechnology, Santa Cruz, Calif.), anti-p21^{CDKN1} mouse monoclonal (Pharmingen, San Diego, Calif.), and β-actin (Sigma Chemical Company, St. Louis, Mo.). The Cdk1 rabbit polyclonal antibody was a kind gift from Dr. Joachim Schnier of the University of California, Davis. After washing, blots were incubated in a 1:10,000 dilution of the appropriate biotinylated secondary antibody (Vector Laboratories, Burlingame, Calif.) for 1 h. Antibodies were detected by incubation with streptavidin-horseradish peroxidase (DAKO Corporation, Carpinteria, Calif.) (1:10,000 dilution in TBST for 30 min) and chemiluminescence detection reagents (ECL, Amersham, Arlington Heights, Ill.). Finally, membranes were exposed to Kodak XAR film, the film developed and the results interpreted.

Growth curves

Cell growth responses to combination CDDP plus UCN-01 were assessed using the MTT assay as previously described [35]. Cells (except controls) were treated with CDDP 1 day after plating. Eight doses of CDDP were tested starting at 50 μM with 50% dilutions down to 0.4 μM. Following CDDP exposure for 3 h, cells were washed and, in triplicate, cells were either treated with UCN-01 or fed fresh medium as CDDP-only controls. The UCN-01 doses used were the previously determined 50% inhibitory concentration (IC_{50}) for each cell line [35]. Cells were treated with UCN-01 for 24 h (A549, Calu1) or 72 h (A549, H596). Cell proliferation was assayed on the 3rd day after initiation of treatment. Signal from the MTT dye was read using an E-max microplate reader and Softmax software (Molecular Devices, Sunnyvale, Calif.).

Median effect analysis

Median effect analysis using the combination index (CI) was employed to determine synergy, additivity, or antagonism (less than additive) of drug combinations [14]. The results from all experiments were pooled and mean values obtained for each data point. This method of determining synergy derives from the mass action law and is independent of mechanism. The median effect equation is given by: $Fa/Fu = (D/Dm)m$, where Fa is the fraction affected, Fu is the fraction unaffected, D is the dose, Dm is the median effect dose and m is the coefficient signifying the shape of the dose response curve ($m = 1$, hyperbolic; $m > 1$ sigmoidal; $m < 1$ negatively sigmoidal). The shape of the curve is easily determined from a plot of dose and effect and rearrangement allows calculation of Dm, the median dose effect also known as the IC_{50}. The CI is defined by the following equation:

$$CI = \frac{(D)1}{(Dx)1} + \frac{(D)2}{(Dx)2}$$

in which (D)1 is the dose necessary for a particular effect in the combination, (Dx)1 is the dose of the same drug which will produce the identical level of effect by itself, (D)2 is the dose of a second drug which will produce a particular effect in the combination and (Dx)2 is the dose of the second drug which will produce the same level of effect by itself. For true combinations, a $CI > 1$ would imply antagonism and a $CI < 1$ would indicate synergy. It should be noted that the CI may vary across drug concentrations so that a particular combination may be antagonistic at one set of concentrations, additive at a second and synergistic at a third. In this situation, the clinically significant effect is usually at the higher drug concentrations. The equation given above is for mutually exclusive drugs, i.e., those with the same mode of action. A third term, (D)1(D)2/(Dx)1(Dx)2, is added if the assumption is that the drugs are mutually non-exclusive, i.e., have completely different modes of action. The mutually non-exclusive assumption is hence more rigorous in its definition of synergy and was employed in these studies. Simplifying this analysis is a computer program (Calcusyn, Biosoft, Ferguson, Mo.) which provides a CI plot and allows easy computation of the Dm (IC_{50}).

Analysis of cell cycling

Cell cycle analysis was performed using flow cytometric evaluation of DNA content. Detached cells in the cultures were collected and combined with attached cells that were harvested by trypsinization. Cells were washed in medium, pelleted, resuspended in 70% ethanol and stored at −20°C. Cells were then centrifuged, washed once in PBS, resuspended in 900 µl PBS with 20 µl DNase-free RNase (Roche Molecular Biochemicals, Indianapolis, Ind.) and incubated at 37°C for 40 min. After incubation, propidium iodide (Boehringer Mannhiem Corporation, Indianapolis, Ind.) was added to a final concentration of 0.05 mg/ml and samples were allowed to stand at room temperature, protected from light, for a minimum of 15 min. Cell aggregates were removed by filtration prior to analysis. Nocodazole (Sigma Chemical Company) was employed to trap cells in M phase. Stock solutions were prepared in DMSO at 50 µg/ml. Final treatment concentrations were 0.1 µg/ml for 24 h. Cell cycle analysis was performed on a Coulter Epics XL flow cytometer (Beckman Coulter, Miami, Fl.). The percentage of cells in each phase of the cell cycle was determined from 50,000 cells with doublet discrimination. Analysis of cell cycle position was done using Phoenix Multicycle software (Phoenix Flow Systems, San Diego, Calif.).

Apoptosis determination

Nuclear morphology was used to assess the process of programmed cell death (apoptosis). One day prior to drug treatment, cells were plated on glass microscope slides (Fisherbrand Superfrost/Plus, Fisher Scientific, Pittsburgh, Pa.) in tissue culture Petri dishes. Cells were fixed 43 h after initiation of treatments using a 4% paraformaldehyde solution for 30 min at room temperature. Cells were stained with 4′,6-diamidine-2′-phenylindole dihydrochloride (DAPI) solution (0.2 µg/ml) (Roche Molecular Biochemicals) with 2% paraformaldehyde and 0.1% Triton-X-100 in PBS for 30 min at 4°C. Mounting medium (Vectashield, Vector Laboratories, Burlingame, Calif.) was applied to the slides, which were then coverslipped. The formation of specific DNA-DAPI complexes results in highly fluorescent nuclei. Slides were viewed under a fluorescent microscope (absorbance 340 nm, emission 488 nm), photographed (ISO 100 35-mm Elite Chrome film; Eastman Kodak, Rochester, N.Y.), and 100 cells per slide in random microscope fields were counted independently by two different operators. The operators were blinded to all treatment groups except controls. Cells that displayed morphology clearly indicative of apoptosis (fragmented nuclei, condensed chromatin) were scored as apoptotic; all other cells were considered non-apoptotic. This procedure likely underestimated the total cell death because cells may have died at other time points or apoptotic cells may have become detached prior to fixation.

Statistics

Statistical comparison of apoptosis data was conducted using one-way analysis of variance (ANOVA) and individual treatments were compared using the Tukey-Kramer Multiple Comparisons test. Statistics were generated using the InStat program, version 3.0 (GraphPad Software, San Diego, Calif.).

Results

Characterization of p53 functional status in NSCLC cell lines

Because some mutant p53 proteins encoded by various cancer-derived alleles have recently been shown to retain

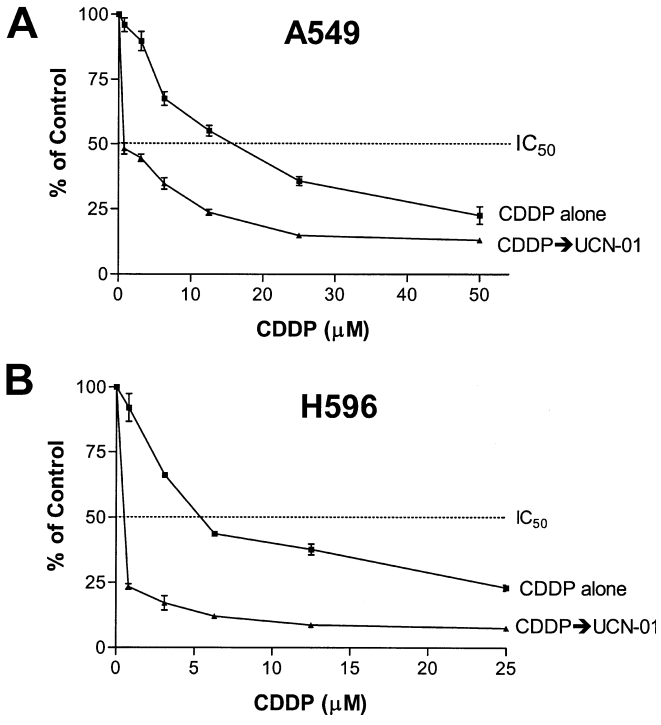

Fig. 1A, B UCN-01 potentiates the activity of CDDP in NSCLC cell lines. Cells were treated 24 h after plating with CDDP for 3 h at concentrations ranging from 0.4 μ*M* to 50 μ*M* and washed. Half of the cultures were left untreated and half were treated with either UCN-01 for 24 h or 72 h at the single-agent IC_{50} dose for each cell line (**A** A549 cells treated with UCN-01 at 250 n*M* for 24 h, **B** H596 cells treated with UCN-01 at 1000 n*M* for 72 h). Cell numbers were quantitated using the MTT assay. Growth inhibition for the treated cultures was plotted as a percentage of the untreated control (*y*-axis). Each experiment was repeated a minimum of two times and representative experiments are shown. *Error bars* indicate standard error of the mean

transactivational function, it was important to characterize the functional status of *p53* in the cells used for our studies. The functional status of *p53* was assessed using a yeast assay that evaluates transactivational activity of proteins encoded by human *p53* alleles. This assay verified the wild-type function of p53 in the A549 cells in our laboratory and determined that the mutant *p53* allele in H596 (codon 245, GGC → TGC, Gly → Cys) demonstrates a total loss-of-function (data not shown) [36]. Calu1 cells are *p53*-null [35].

UCN-01 potentiates CDDP activity

To investigate the effects of UCN-01 on CDDP anticancer activity, the growth characteristics of NSCLC cell lines A549 (wt *p53*; wt *RB*) and H596 (mt *p53*; *RB*-null) were assessed after treatment with various concentrations of CDDP (up to 50 μ*M*) in the presence or absence of UCN-01 at the IC_{50} of UCN-01 for each individual cell line as determined from our earlier work (A549 250 n*M*, H596 1000 n*M*; Fig. 1) [35]. In these experiments, 3-h CDDP treatments preceded UCN-01 treatments and cells were harvested at 24 h or 72 h. In all cell lines, the addition of UCN-01 as the second drug potentiated the response induced by CDDP, and this was seen regardless of the length of UCN-01 treatment and irrespective of either *p53* or *RB* status. For Calu1 cells, a 24-h incubation with UCN-01 was sufficient to reduce the CDDP IC_{50} to below 0.4 μ*M* (the lowest CDDP dose used). For A549 and H596, 72-h UCN-01 treatments resulted in equivalent reductions. IC_{50} values for the combination drug treatments from these experiments are listed in Table 1.

Table 1 Potentiation of CDDP by UCN-01. Cells were treated with CDDP followed immediately by UCN-01 for 24 h (Calu1, A549) or 72 h (A549, H596). Shown are CDDP concentrations (μ*M*) required to achieve a 50% growth inhibition (IC_{50}). The addition of UCN-01 (for 24 h or 72 h) substantially reduced CDDP IC_{50}

Treatment	IC_{50} (μ*M*)		
	Calu1	A549	H596
CDDP alone	10	15	5
CDDP → UCN-01			
24 h UCN-01	< 0.4	1.5	–
72 h UCN-01	–	< 0.4	< 0.4

Potentiation of CDDP by UCN-01 is dependent on the sequence of drug administration

Median effect analysis was conducted to determine the nature of drug interactions and whether the interactions were sensitive to the timing of administration of the two drugs. In A549 cells, when UCN-01 preceded CDDP, the drug interaction was predominantly antagonistic (less than additive) (Fig. 2A); however, when the order of drug administration was reversed (CDDP → UCN-01), the combination effect was predominantly synergistic (Fig. 2B). Similar sequence effects were seen with H596 cells, demonstrating that the sequence of drug administration is important for response (Fig. 2C, D).

Treatment schedule for the evaluation of cell cycle and apoptotic responses

For the following studies, we adopted a treatment schedule that would allow cells the necessary time to achieve cell cycle arrest at specific checkpoints prior to addition of the second agent (Fig. 3). A UCN-01 dose of 100 n*M* for 24 h was chosen because of its ability to modulate cell cycling with minimal cytotoxicity, as shown in several previous studies [8, 35, 56]. CDDP was administered for 3 h at the IC_{50} for each cell line (see above) followed by a 16-h drug-free interval to allow sufficient time for the majority of cells to arrest following CDDP-induced DNA damage. This treatment was then followed by either UCN-01 (24 h) or, for the CDDP single-agent treatments, a further 24-h drug-free interval.

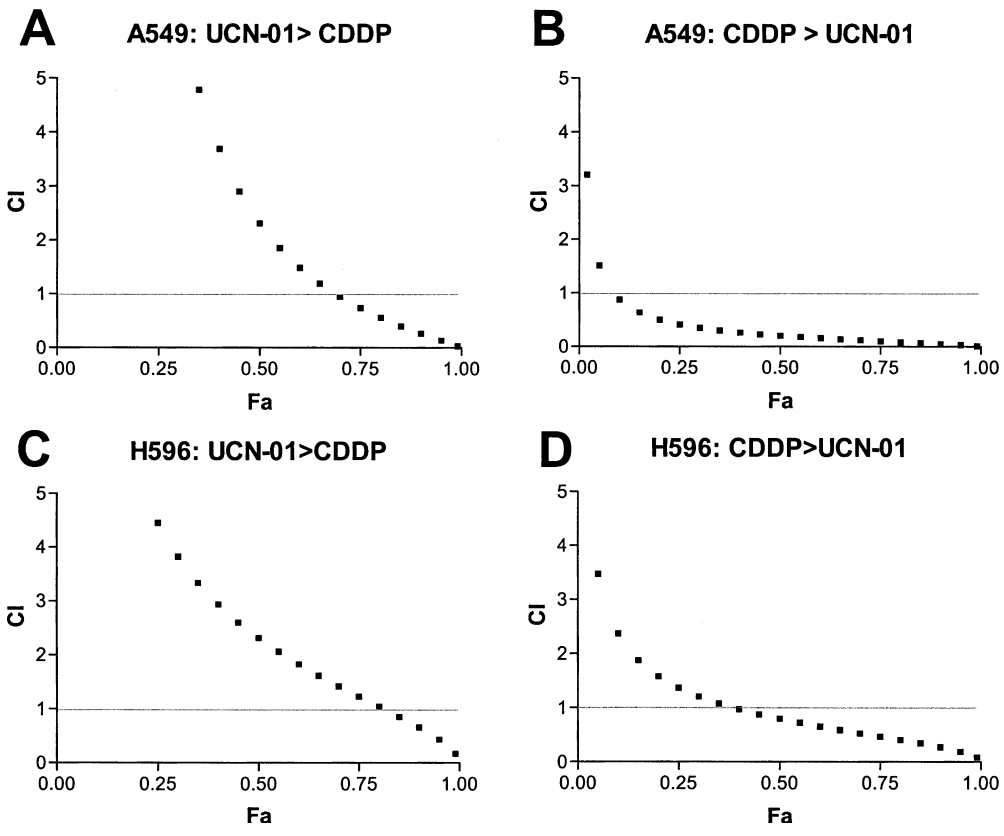

Fig. 2A–D Degree of drug interaction is dependent on sequence of drug administration. Median effect analysis was used to determine whether the interaction between CDDP and UCN-01 was synergistic, additive or antagonistic. A combination index (CI) of 1, indicated on each graph by a horizontal line, represents an additive interaction. CI values >1 are antagonistic (less than additive); CI values <1 are synergistic (supra-additive). *Fa* fraction affected, indicating the ratios of increasing drug concentrations. **A C** UCN-01 treatment for 24 h prior to CDDP for 3 h (*UCN-01 > CDDP*), **B D** CDDP treatment for 3 h prior to UCN-01 for 24 h (*CDDP > UCN-01*)

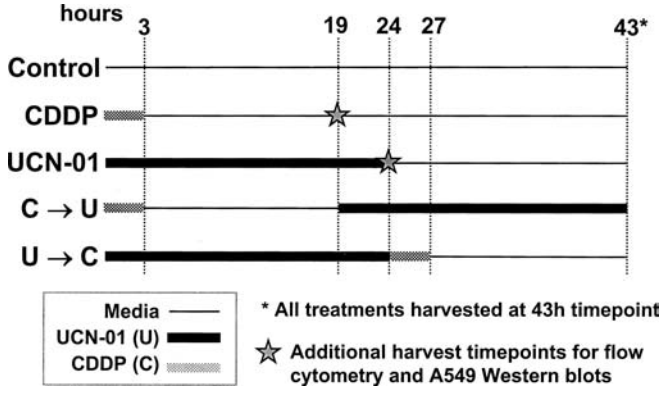

Fig. 3 Treatment schedule for cell cycle, protein expression and apoptosis analyses. As indicated, both single-agent and combination treatments were 43 h in duration (*hatched gray lines* CDDP, *thick black lines* UCN-01, *thin black lines* medium alone). For single-agent CDDP treatments, cells were incubated with CDDP for 3 h followed by 40 h in media alone. For single-agent UCN-01 treatments, cells were incubated with UCN-01 for 24 h followed by 19 h in medium alone. In combination treatments, CDDP for 3 h plus 16 h drug-free was preceded by 24 h UCN-01 ($U \rightarrow C$) or followed by 24 h UCN-01 ($C \rightarrow U$). Additional single-agent time points were included for the flow cytometric analysis of A549 and Calu1 cells and for the Western blot analysis of A549 cells. These additional harvests (*large stars*) were after CDDP for 3 h followed by 16 h drug-free or after UCN-01 for 24 h, and represent the status of cells at the point where the second drug would be administered in a combination treatment

Alternatively, UCN-01 treatments (24 h) were followed by CDDP (3 h plus 16 h drug-free) or 19 h drug-free for single-agent studies. Thus, all treatments, whether single-agent or combination, were harvested at the same time point (43 h) after initiation of treatment. Additional harvest time points for single-agent treatments were immediately after 24 h of UCN-01 or at the 19-h time point, as indicated in Fig. 3 by large stars. These were done to document the cell cycle position and molecular responses of cells at the time point when the second drug was introduced.

Cell cycle effects of CDDP plus UCN-01

The cell cycle modulatory effects of combination treatments with CDDP plus UCN-01 were investigated and compared with those of each agent alone. The effects of single-agent UCN-01 (100 n*M*) were examined in A549 and Calu1 cells. For both cell lines, UCN-01 treatment for 24 h resulted in an increase of cells in G_1 phase compared to untreated cells (Fig. 4, U versus Control). This G_1 arrest was reversible as evidenced by the increased S phase observed 19 h after UCN-01 was washed out (Fig. 4, $U \rightarrow M$).

Treatment with single-agent CDDP (3 h CDDP plus 16 h drug-free) resulted in the accumulation of cells predominantly in G_2/M in A549 cells and predominantly in S phase in Calu1 cells (Fig. 4, C). After an additional 24-h drug-free incubation (at the 43-h time point), the majority of cells from both lines had progressed into G_2/M (Fig. 4, $C \rightarrow M$). At this time point, a substantial proportion of A549 cells were in G_1 phase in contrast to Calu1 cells which had very few G_1 cells.

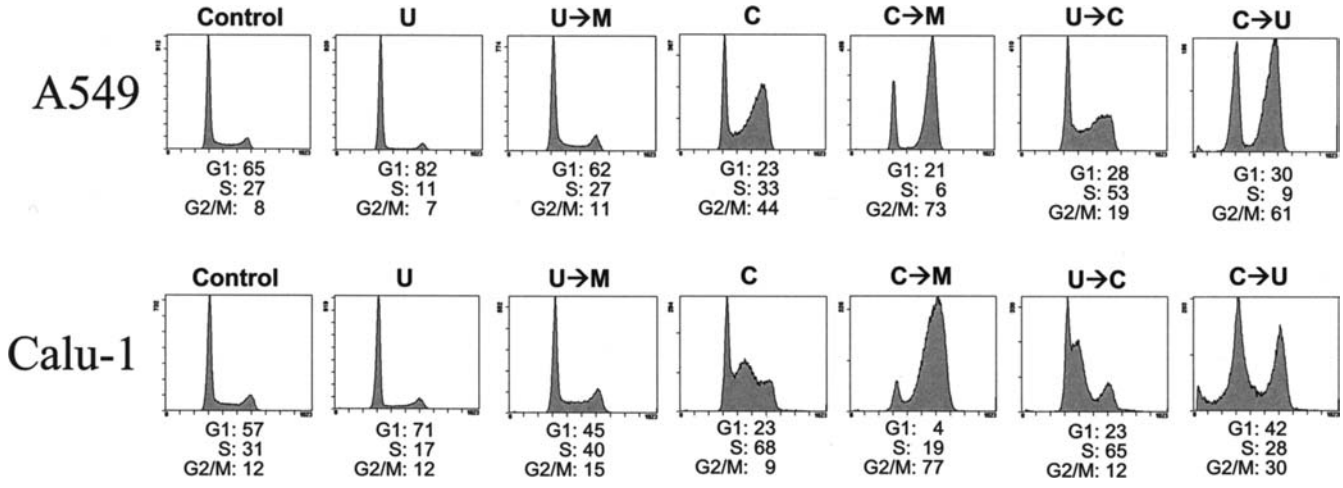

Fig. 4 Cell cycling effects of CDDP plus UCN-01 in A549 and Calu1 cells. The results of representative experiments are shown detailing cell cycle distribution as measured by flow cytometric analysis of DNA content after treatment with CDDP and UCN-01 as single agents or in sequential combinations, using the treatment schedule illustrated in Fig. 3. *X-axis* DNA content, *Y-axis* number of cells. *Control* no drug treatment, *U* 24 h UCN-01, *U* → M 24 h UCN-01 followed by 19 h drug-free medium, *C* 3 h CDDP followed by 16 h drug-free medium, *C* → M 3 h CDDP followed by 40 h drug-free medium, *U* → C 24 h UCN-01 followed by 3 h CDDP followed by 16 h drug-free medium, *C* → U 3 h CDDP followed by 16 h drug-free medium followed by 24 h UCN-01

This is consistent with their *p53* status (A549 wt *p53*, Calu1 *p53*-null) and the well-established role of p53 in DNA damage-induced G_1 arrest.

Combination treatments were conducted in alternate sequences as shown diagrammatically in Fig. 3. The treatment sequence of UCN-01 followed by CDDP (Fig. 4, U → C) resulted in increased S phase with limited G_2/M accumulation. Cell cycle histograms in this sequence were similar to those of CDDP at the 19-h time point (Fig. 4, C) but with what appears to be a slight lag in cell cycle progression, likely resulting from pretreatment with UCN-01. When CDDP preceded UCN-01 (Fig. 4, C → U), a decrease in the proportion of cells accumulated in G_2/M was seen in contrast to the cells treated with CDDP followed by an equivalent time in drug-free medium (Fig. 4, C → M). In Calu1 cells, the population shift from G_2/M to G_1 was substantially greater than that found in A549 cells. This G_1 phase increase may have resulted from a UCN-01-mediated abrogation of the CDDP-induced DNA damage checkpoint. It is important to keep in mind that cells that have died are no longer represented in the remaining populations.

A third cell line, H596 (mutant *p53*, *RB*-null), was also examined for the cell cycle effects of CDDP and UCN-01 (Fig. 5). In these experiments, all cells were harvested at the 43-h time point. Treatment with single-agent UCN-01 had no observable effect on cell cycle progression (Fig. 5, U → M), whereas treatment with single-agent CDDP resulted in accumulation in S and G_2/M (Fig. 5, C → M). When CDDP was followed by UCN-01 (Fig. 5, C → U), the proportion of cells in G_1 was increased compared to single-agent CDDP, consistent with the results with the other two cell lines.

The presence of cells with a sub-G_1 DNA content is an indicator of cell death by apoptosis. The treatment sequence of CDDP followed by UCN-01 (Figs. 4 and 5, C → U) resulted in the accumulation of cells with a sub-G_1 content in all three cell lines that was not observed (or minimally so) in cells treated with CDDP alone (Figs. 4 and 5, C → M) or in the reverse sequence (Figs. 4 and 5, U → C). The proportion of sub-G_1 content was

Fig. 5 Cell cycling effects of CDDP plus UCN-01 in H596 cells. The results of representative flow cytometric analyses are shown detailing cell cycle distribution of H596 cells after treatment with CDDP and UCN-01 as single agents or in sequential combinations, using the treatment schedule illustrated in Fig. 3. *X-axis* DNA content, *Y-axis* number of cells. *Control* no drug treatment, *U* → M 24 h UCN-01 followed by 19 h drug-free medium, *C* → M 3 h CDDP followed by 40 h drug-free medium, *U* → C 24 h UCN-01 followed by 3 h CDDP followed by 16 h drug-free medium, *C* → U 3 h CDDP followed by 16 h drug-free medium followed by 24 h UCN-01

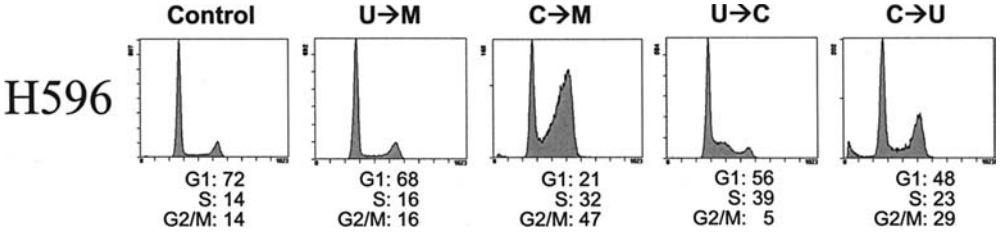

Table 2 Apoptosis, as measured by sub-G_1 DNA content, is evident only with the C → U sequence. The sub-G_1content was measured in flow cytometry histograms (Figs. 4 and 5) using vertical gating.Shown are the percentages of cells with a DNA content less than that of the G_1 peak after doublet discrimination.Minimal levels of sub-G_1content, ranging from 0.29 to 1.47%, were observed in controls, and with the single-agent treatments (U → M and C → M) and the U → C sequence. Substantially increased percentages were observed when CDDP preceded UCN-01 (C → U)

Cell line	Control	U → M	C → M	U → C	C → U
A549	0.33	0.29	0.56	0.47	3.42
Calu1	1.06	1.36	1.29	1.42	13.85
H596	1.37	0.49	1.47	0.71	8.86

substantially greater in both cell lines with dysfunctional *p53* (Calu1 and H596) than in A549 cells (Table 2).

Abrogation of the CDDP-induced DNA damage checkpoint arrest is evident in Calu1 cells but not in A549 cells

As noted above, the percentages of cells in G_1 were increased in cells treated with CDDP followed by UCN-01 as compared to CDDP followed by drug-free medium. To investigate the origin of these G_1 populations in A549 and Calu1 cells, the mitotic inhibitor nocodazole was used in a mitotic trapping assay. Since nocodazole is an antimicrotubule agent, cells are trapped in M phase and cell division is prevented. Thus, nocodazole treatment can be used to discriminate cells that divide and repopulate G_1 from those that remain in G_1 as a result of the initial treatment. Figure 6 shows the consequence of a 24-h incubation with nocodazole in A549 and Calu1 cells. Nocodazole alone (Fig. 6, N) resulted in accumulation of cells in G_2/M for both cell lines. When cells were coincubated with UCN-01 and nocodazole for 24 h (Fig. 6, U + N), a difference between the two cell lines emerged: 20% of A549 cells remained in G_1 phase, whereas only 5% of Calu1 cells remained in G_1. Thus, in A549 cells, UCN-01 treatment resulted in an initial G_1 arrest that was maintained for a substantial fraction of cells throughout the 24-h treatment. Similarly, comparison of the G_1 content of cells treated with CDDP followed by nocodazole for 24 h (Fig. 6, C → N) with cells treated with CDDP followed by a simultaneous 24-h administration of UCN-01 and nocodazole (Fig. 6, C → U + N) revealed that a substantial proportion of A549 cells remained in G_1, but this was not observed in Calu1 cells. These results indicate that, in Calu1 cells, the increase in G_1 content observed in the C → U compared to the C → M sequence in Fig. 4 cannot be accounted for by an initial drug-induced G_1 arrest. This demonstrates that UCN-01 treatment is abrogating the CDDP-induced G_2 arrest. In contrast, in A549 cells, the increase in G_1 cells observed in C → U was likely not due to a UCN-01-mediated abrogation of the CDDP checkpoint, but instead due to a drug-induced G_1 arrest.

UCN-01 treatment reactivates Cdk1 leading to exit from CDDP-induced G_2 arrest

In response to DNA-damaging agents such as CDDP, Cdk1 is inhibited by phosphorylation at Thr14 and Tyr15, characterized by a lag in the electrophoretic

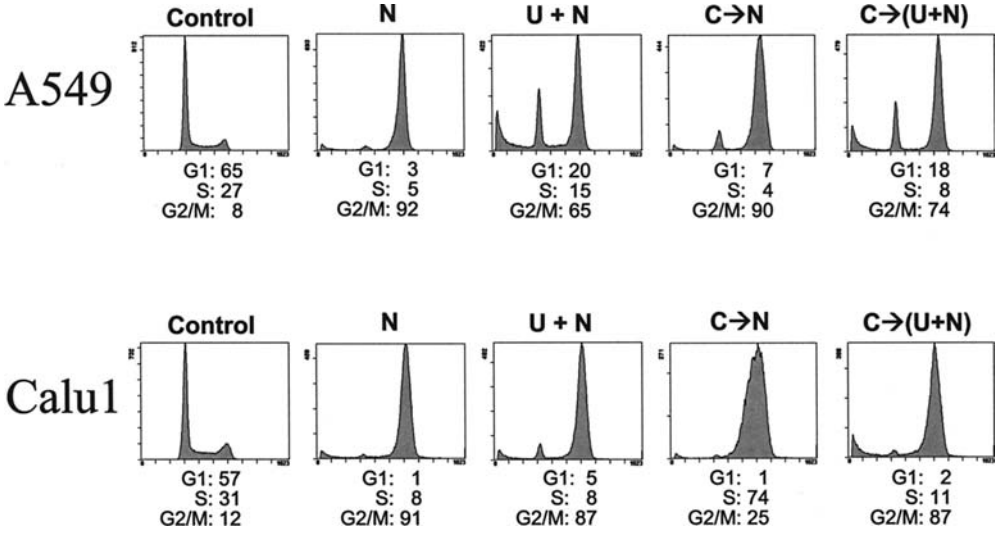

Fig. 6 Mitotic trapping demonstrates UCN-01-mediated abrogation of the CDDP-induced checkpoint arrest in Calu1 cells but not A549 cells. Nocodazole was used to determine whether G_1 cells were from CDDP- or UCN-01-induced G_1 arrest or by repopulation of G_1 during the course of treatment. *N* nocodazole for 24 h, *U + N* simultaneous 24 h incubation with UCN-01 and nocodazole, *C* → N 3 h CDDP followed by 16 h drug-free medium followed by 24 h nocodazole, *C* → (U + N) 3 h CDDP followed by 16 h drug-free medium followed by simultaneous 24 h incubation with UCN-01 and nocodazole. In Calu1 cells, mitotic trapping prevented repopulation of G_1, whereas in A549 cells, this experiment revealed the presence of an initial and durable G_1 arrest in UCN-01-containing treatments

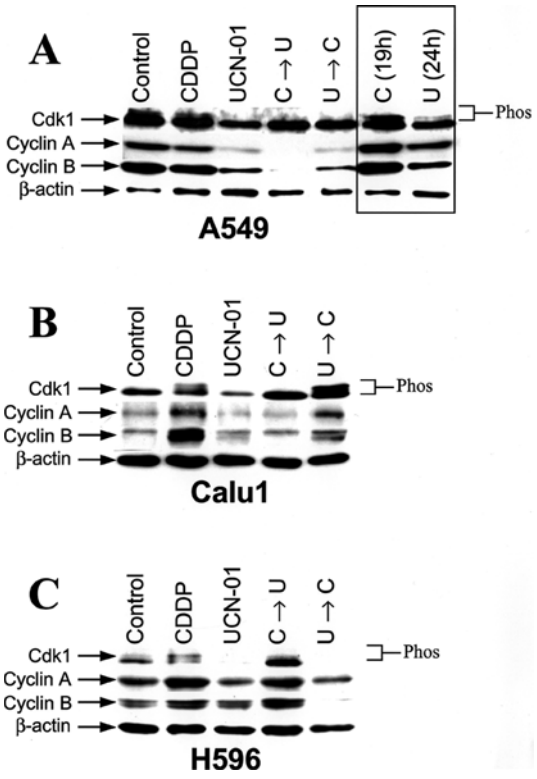

Fig. 7A–C Changes in Cdk1 phosphorylation and cyclins A and B levels in NSCLC cells after treatment with UCN-01 and CDDP. Western blot analysis was performed to assess changes in levels of cyclins A and B and phosphorylation of Cdk1, using β-actin as an endogenous standard. For Cdk1, the presence of bands migrating more slowly is indicative of inhibitory protein phosphorylation (*phos*). **A** A549 cells: the lanes in the box, labeled *C (19h)* and *U (24h)*, show the status of the proteins from cells harvested immediately after the 3 h CDDP plus 16 h drug-free medium (i.e., immediately prior to the addition of UCN-01) and after 24 h UCN-01 (i.e., immediately prior to the addition of CDDP), respectively. **B** Calu1 cells; **C** H596 cells

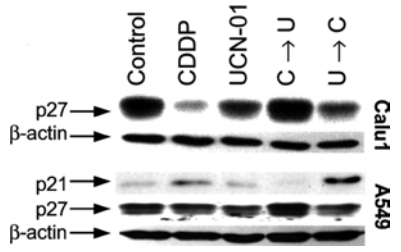

Fig. 8 p27 accumulation after treatment with CDDP followed by UCN-01. Western blot analysis was used to assess changes in levels of the Cdk inhibitor p27 in the *p53*-null Calu1 cell line, and both p21 and p27 in A549 cells (wt *p53*) using the treatment schedule illustrated in Fig. 3. β-actin was used as the endogenous standard control

mobility of the protein. On the other hand, treatment with UCN-01, via inhibition of the Chk1 pathway, can return Cdk1 to an activated state. As a marker of biological activities of both drugs, the phosphorylation state of Cdk1 was evaluated by Western blot analysis. Because cyclin A is elevated in S and G_2 phases, and cyclin B is elevated in G_2 and M phases, protein levels of these cyclins were examined to further define cell cycle position in response to treatment. These experiments used the 43-h treatment schedule illustrated in Fig. 3, with the inclusion of two additional early time points for A549 that represent the status of the cells after treatment with the initial drugs (CDDP 19 h, UCN-01 24 h). In response to CDDP as a single agent, Cdk1 showed the expected presence of bands migrating more slowly, indicating inhibitory phosphorylation of the protein, and the levels of both cyclins A and B were elevated (Fig. 7). Here, the proteins were consistent with the observed G_2/M accumulation with a substantial portion in G_2 as indicated by the elevated cyclin A levels. Similar results were observed with all three cell lines; however in A549 cells, CDDP-induced Cdk1 phosphorylation and increased cyclin A and B levels were more evident at the 19-h time point (16 h after removal of CDDP), as shown in Fig. 7A, lane C(19h). Following the UCN-01 → CDDP treatment, Cdk1 inhibitory phosphorylation was absent, and levels of both cyclins A and B were diminished, consistent with the reduction in the percentage of cells in G_2/M seen by flow cytometry.

UCN-01 as a single agent (24 h UCN-01 followed by 19 h drug free) resulted in levels of cyclins A and B similar to those of control cultures, as expected from the transient effect of the 100-n*M* dose on cell cycling. Single-agent UCN-01 also resulted in reduced levels of Cdk1 in all three cell lines, which may be related to decreased cellular content of Cdk1 in G_1 phase [58]. In the UCN-01 → CDDP sequence, phosphorylated Cdk1 and moderate increases in cyclin A were observed in Calu1 cells, consistent with S-phase accumulation. However, in A549 and H596 cells, these effects were not observed at the time point examined.

Levels of the Cdk inhibitors p27 and p21 were assessed in Calu1 and A549 cells after treatment with CDDP and UCN-01 (Fig. 8). UCN-01 as a single agent has been previously shown to induce both p21 and p27, independently of *p53* [5, 33, 35]. Our previous work showed that 500 n*M* of UCN-01 is sufficient to induce p21 expression in Calu1 cells (*p53*-null) [35]. In the present study, basal levels of p21 were nearly undetectable in Calu1 cells and treatment with either UCN-01 (100 n*M*) or CDDP did not result in any noticeable increase (data not shown). In A549 cells, in response to UCN-01 as a single agent, p21 was induced at 24 h [35], but was diminished after further incubation in drug-free medium (at the 43-h time point), indicating the transient nature of the molecular response to this dose of UCN-01 in these cell lines [49]. Expression of p21 increased after CDDP treatment, but was sharply reduced in the CDDP → UCN-01 sequence. In contrast, levels of p27 were reduced in single-agent CDDP treatments, likely reflecting the accumulation of cells beyond G_1 where p27 levels decrease. However, in cells treated with UCN-01 after CDDP, p27 levels rebounded to control levels or higher.

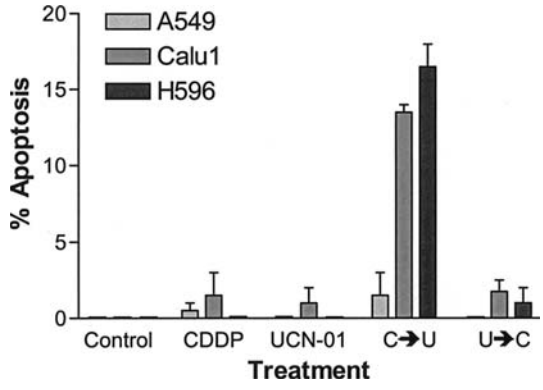

Fig. 9 Apoptosis resulting from CDDP and UCN-01 is dependent on sequence of drug administration and is more pronounced in NSCLC cells with dysfunctional *p53*. Assessment of nuclear morphology was used to measure the extent of apoptosis in NSCLC cell lines using the treatment schedules illustrated in Fig. 3. Shown are the averages of counts from two independent experiments. *Error bars* indicate standard error of the mean. In Calu1 cells (*p53*-null) and H596 cells (mt *p53*), the CDDP → UCN-01 sequence (*C* → U) resulted in a statistically significant increase in apoptosis (ANOVA, $P < 0.0001$ for both cell lines). In A549, no significant differences were seen with any treatment, although apoptosis levels were slightly elevated in the CDDP → UCN-01 sequence (*C* → U)

UCN-01 after CDDP, but not the reverse schedule, results in increased apoptosis, particularly in cell lines with dysfunctional *p53*

Analysis of the sub-G_1 DNA content in the DNA histograms (Figs. 4 and 5) provided a preliminary assessment of apoptosis, and indicated that the sequence CDDP → UCN-01 may be the most effective. As a further assessment of apoptosis, condensed chromatin within nuclei or highly fragmented nuclei were scored to determine the impact of UCN-01-induced checkpoint abrogation on cell death at the 43-h time point (Fig. 9). Little apoptosis was observed at this time point with CDDP or UCN-01 as single agents. Similarly, minimal apoptosis (less than 2%) was observed in all cell lines when treated with the UCN-01 → CDDP sequence. In sharp contrast, apoptosis was prevalent with the CDDP → UCN-01 sequence in cells with disrupted *p53*. These observations are consistent with the amount of sub-G_1 DNA content observed by flow cytometry (summarized in Table 2).

Discussion

We examined the effects of two-drug treatments with CDDP plus the checkpoint abrogator UCN-01 using three NSCLC lines with different molecular status of the *p53* and *RB* genes. UCN-01 treatment resulted in a timing-specific enhancement of the anticancer effects of CDDP, with the regimen CDDP followed by a 16-h drug-free interval and then 24 h of UCN-01 shown to be more effective. In addition to the results of the present study, other studies have demonstrated that UCN-01 can enhance the antitumor effectiveness of a wide array of DNA-damaging agents, and it is anticipated that UCN-01 will achieve its greatest clinical utility in this setting [3, 8, 31, 35, 38, 54, 56]. Potentiation of DNA damagers by UCN-01 is thought to stem, at least in part, from its ability to abrogate S and G_2 phase DNA damage-induced checkpoint arrests, although this has not always been definitively demonstrated [8, 9, 31, 34, 55, 56]. UCN-01, at low to medium nanomolar concentrations, has an array of targets that may influence its clinical utility in a combination setting. These include inhibition of PKC and G_1 phase Cdks, induction of Cdk inhibitors, and proteolytic degradation of E2F, each of which can contribute to G_1 arrest [2, 5, 28, 32, 35, 45, 52, 55]. While these activities could lead to cytostatic tumor growth inhibition, in a two-drug setting they may interfere with the potentiation activity of UCN-01 that results from checkpoint abrogation.

Progression through the G_2 checkpoint is principally regulated by Cdk1 and cyclin B. In response to DNA damage, the checkpoint kinase Chk1 inactivates the Cdc25C phosphatase via phosphorylation of Ser-216, resulting in Cdc25C complex formation with 14-3-3 protein and subsequent sequestration into the cytoplasm [22, 41, 45, 46]. When inactive, Cdc25C can no longer remove Thr-14 and Tyr-15 phosphorylation on Cdk1, resulting in the accumulation of this inhibitory phosphorylation, and G_2 checkpoint arrest. It has recently been shown mechanistically that UCN-01 disrupts G_2 checkpoint arrest by inhibiting Chk1 protein kinase activity [11, 25]. After DNA damage, this inhibition of Chk1 prevents inactivation of Cdc25C, resulting in removal of the inhibitory phosphorylation from Cdk1 and promotion of premature entry into M phase.

In the present study, UCN-01 treatment resulted in a sequence-specific enhancement of CDDP activity. When CDDP preceded UCN-01, the drug interaction was synergistic in all three NSCLC cell lines examined. CDDP as a single agent induced a G_2 arrest coincident with inhibitory phosphorylation of Cdk1 and increased levels of cyclins A and B. Subsequent treatment with UCN-01 resulted in a relative increase in G_1 content associated with a complete loss of the CDDP-mediated Cdk1 inhibitory phosphorylation, consistent with the activity of UCN-01 as a G_2 checkpoint abrogator. Decreased levels of both cyclins A and B and increased levels of p27 provide further evidence of UCN-01-mediated G_2 arrest abrogation. Experiments with the mitotic inhibitor nocodazole confirmed that, in the *p53*-null Calu1 cell line, the increased percentage of G_1 cells was not due to an immediate UCN-01- or CDDP-mediated G_1 arrest, but was a result of a later repopulation of G_1. This sequence of CDDP followed by UCN-01 was also associated with significant rates of apoptosis in the two *p53*-compromised cell lines, compared to either single-agent treatment or to the reverse sequence (UCN-01 preceding CDDP). Taken together, these results indicate that the potentiation of CDDP cytotoxicity by UCN-01 results primarily from G_2 checkpoint arrest

abrogation, and is most pronounced in cells with a compromised *p53*.

It has recently been shown that in addition to G_1 arrest, wt *p53* contributes to the maintenance of G_2 arrest following DNA damage through an alternative to the Chk1 pathway. Thus, it would be anticipated that cells with dysfunctional *p53* would be more susceptible to checkpoint abrogation by a UCN-01-directed inhibition of the *p53*-independent Chk1 pathway [10, 50]. Wang et al. have demonstrated, using an MCF-7 model transfected with the human papillomavirus type-16 *E6* gene, that cells with disrupted p53 are more sensitive to UCN-01-mediated checkpoint abrogation and have reduced colony forming ability [56]. While the findings of several studies are in agreement with these *p53* findings, others have produced discrepant results [27, 29]. In our study, NSCLC cells with abnormal *p53* (Calu1 *p53*-null, H596 mt *p53*) demonstrated markedly increased apoptosis when UCN-01 was administered after CDDP, suggesting the potential value of this treatment for NSCLC in which *p53* is frequently disrupted [13, 37].

In A549 cells, which have wt *p53*, abrogation of the G_2 DNA damage checkpoint could not be conclusively demonstrated. In this line, the large G_1 population when CDDP was followed by UCN-01 may have been due to cells being trapped in G_1 by CDDP and/or UCN-01, as demonstrated by the studies with nocodazole (Fig. 6). Apoptosis, as measured by increased sub-G_1 DNA content and by altered nuclear morphology, was slightly and consistently elevated in A549 cells in the CDDP → UCN-01 sequence, although not to a statistically significant level.

The potential role of the *RB* gene was of interest to us because of our previous findings that wt *RB* contributes to UCN-01-induced G_1 arrest [35]. In that study, the *RB*-null cell line H596 was essentially refractory to the growth-inhibitory effects of low-dose UCN-01 as a single agent. Despite this, H596 cells responded dramatically to treatment with CDDP followed by UCN-01, indicating that disrupted *RB* factors little into the response to this sequence. Considering the high frequency of disrupted *RB* in small-cell lung cancer (SCLC) [26], this tumor type may be an ideal candidate for this combination in the demonstrated sequence, as opposed to treatments with single-agent UCN-01 that are *RB*-dependent.

Our studies with UCN-01, as a single agent and in combination with CDDP, suggest a general model to explain the varied responses seen with the alternate sequences of CDDP plus UCN-01, related to the cell cycle and the status of tumor suppressor genes *RB* and *p53* (Fig. 10). When UCN-01 is administered prior to CDDP, *RB*-competent cells accumulate in G_1 in response to UCN-01. This activity results in a reversible cytostatic response that potentially limits CDDP -induced cytotoxicity in other phases of the cell cycle.

When CDDP is administered first, cells accumulate at DNA damage checkpoints and attempt to repair CDDP-mediated DNA adducts and intrastrand crosslinking. The addition of UCN-01 to cells that have checkpoint arrested in either S or G_2, by reducing the period of DNA damage-induced arrest, acts adversely to DNA repair. Reduced repair time likely contributes to a lethal failure to repair DNA damage and an increased propensity for apoptosis, thereby potentiating CDDP. This is accentuated in cells lacking functional *p53*, where both G_1 and G_2 checkpoint arrests are compromised. At the G_2 checkpoint, DNA damage induces arrest through both *p53*-dependent and *p53*-independent mechanisms. Thus, the lack of functional *p53* removes one level of regulation, rendering these cells more vulnerable to UCN-01 inhibition of the *p53*-independent Chk1 pathway. Additionally,

Fig. 10 Model of sequence effects of combination CDDP plus UCN-01. Treatment with UCN-01 prior to CDDP (*left-hand diagram*) would be expected to result in an *RB*-influenced, UCN-01-mediated predominantly cytostatic response that may serve to minimize apoptosis from CDDP due to accumulation of cells in G_1 phase. In the CDDP → UCN-01 sequence (*right-hand diagram*), cytotoxicity resulting from CDDP-induced DNA damage is potentiated by the addition of UCN-01 to cells arrested at the S and G_2 checkpoints. UCN-01 accelerates exit from these checkpoints, reducing DNA repair and increasing cell death, which is more pronounced in cells with disrupted *p53*

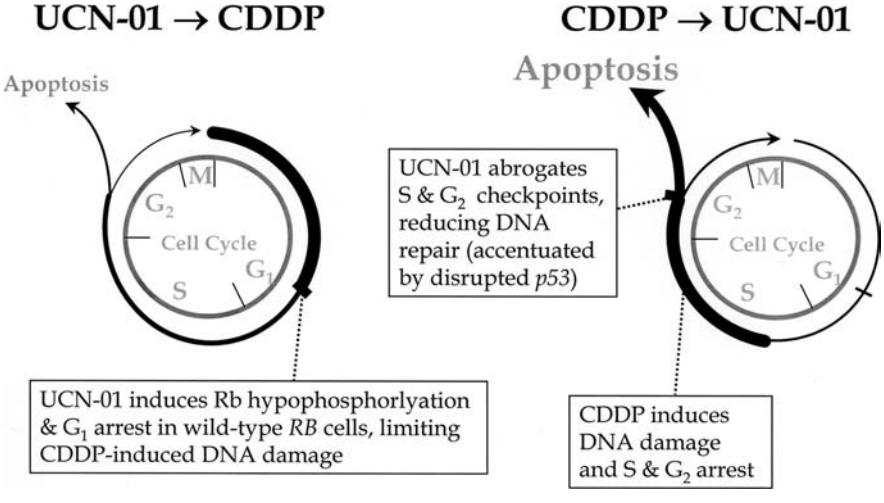

Jiang and Yang have shown that UCN-01 can suppress DNA repair of CDDP-induced DNA damage via attenuation of *XPA-ERCC1*-associated nucleotide excision repair activity [30], which also may contribute to the sequence-dependent response seen here.

An important issue regarding UCN-01 has been the availability of free drug in the plasma of patients and the relationship to doses used in in vitro studies like this one. In a phase I trial of UCN-01 conducted by the NCI, the half-life of UCN-01 was found to be considerably increased in humans compared to that in rats and dogs [47]. It was subsequently discovered that UCN-01 binds avidly to human α_1-acid glycoprotein (hAGP), resulting in high plasma concentrations and a reduction in UCN-01 distribution and clearance [23, 24, 47]. Analysis of salivary UCN-01 concentrations suggested that sustained free drug concentrations in excess of the ones used in this study (100 n*M*) are achievable with doses administered to human patients [47, 48].

As a result of several studies, including the one presented here examining sequence and timing issues of this combination treatment, NCI-sponsored phase I clinical trials have been initiated within the California Cancer Consortium and at Dartmouth University using the sequence of CDDP followed on the subsequent day by UCN-01. Molecular correlative studies to be performed on serial patient tumor biopsies in conjunction with these trials are likely to provide additional information regarding the response consequences of this regimen. Another NCI-sponsored Phase I trial predicated upon this work utilizes the closely related agent carboplatin. This study, at the University of Maryland, evaluates the regimen of carboplatin followed by UCN-01.

In conclusion, molecularly targeted anticancer agents such as UCN-01 hold great clinical promise for lung cancer, particularly in combination with traditional chemotherapies. Optimal application of such agents in a combination setting will require a detailed understanding of (1) the effects of these agents on cell cycling, (2) the relationship between the position of cells in the cell cycle and the response to the agent, (3) the effects of specific cancer mutations on response, and (4) the sequence and timing of drug administration.

Acknowledgements The authors thank Matthew H. Gustafsson for his expert assistance with the flow cytometry, William S. Holland for performing the yeast *p53* functional assays, Susan L. Scott for her helpful discussions and for her assistance with the apoptosis assay, and Nancy J. Nesslinger for editorial assistance and technical advice.

References

1. Aguda BD (1999) A quantitative analysis of the kinetics of the G2 DNA damage checkpoint system. Proc Natl Acad Sci USA 96:11352
2. Akinaga S, Gomi K, Morimoto M, Tamaoki T, Okabe M (1991) Antitumor activity of UCN-01, a selective inhibitor of protein kinase C, in murine and human tumor models. Cancer Res 51:4888
3. Akinaga S, Nomura K, Gomi K, Okabe M (1993) Enhancement of antitumor activity of mitomycin C in vitro and in vivo by UCN-01, a selective inhibitor of protein kinase C. Cancer Chemother Pharmacol 32:183
4. Akinaga S, Nomura K, Gomi K, Okabe M (1994) Effect of UCN-01, a selective inhibitor of protein kinase C, on the cell-cycle distribution of human epidermoid carcinoma, A431 cells. Cancer Chemother Pharmacol 33:273
5. Akiyama T, Yoshida T, Tsujita T, Shimizu M, Mizukami T, Okabe M, Akinaga S (1997) G1 phase accumulation induced by UCN-01 is associated with dephosphorylation of Rb and CDK2 proteins as well as induction of CDK inhibitor p21/cip1/WAF1/Sdi1 in p53-mutated human epidermoid carcinoma A431 cells. Cancer Res 57:1495
6. Albain KS, Crowley J, LeBlanc M, Livingston R (1991) Survival determinants in extensive stage non-small cell lung cancer: the Southwest Oncology Group experience. J Clin Oncol 9:1618
7. Bulavin DV, Amundson SA, Fornace AJ (2002) p38 and Chk1 kinases: different conductors for the G(2)/M checkpoint symphony. Curr Opin Genet Dev 12:92
8. Bunch RT, Eastman A (1996) Enhancement of cisplatin-induced cytotoxicity by 7-hydroxystaurosporine (UCN-01), a new G2-checkpoint inhibitor. Clin Cancer Res 2:791
9. Bunch RT, Eastman A (1997) 7-Hydroxystaurosporine (UCN-01) causes redistribution of proliferating cell nuclear antigen and abrogates cisplatin-induced S-phase arrest in Chinese hamster ovary cells. Cell Growth Differ 8:779
10. Bunz F, Dutriaux A, Lengauer C, Waldman T, Zhou S, Brown JP, Sedivy JM, Kinzler KW, Vogelstein B (1998) Requirement for p53 and p21 to sustain G2 arrest after DNA damage. Science 282:1497
11. Busby EC, Leistritz DF, Abraham RT, Karnitz LM, Sarkaria JN (2000) The radiosensitizing agent 7-hydroxystaurosporine (UCN-01) inhibits the DNA damage checkpoint kinase hChk1. Cancer Res 60:2108
12. Chan TA, Hwang PM, Hermeking H, Kinzler KW, Vogelstein B (2000) Cooperative effects of genes controlling the G2/M checkpoint. Genes Dev 14:1584
13. Chiba I, Takahashi T, Nau MM, D'Amico D, Curiel DT, Mitsudomi T, Buchhagen DL, Carbone D, Piantadosi S, Koga H, Reissman PT, Slamon DJ, Holmes EC, Minna JD (1990) Mutations in the p53 gene are frequent in primary, resected non-small cell lung cancer. Lung Cancer Study Group. Oncogene 5:1603
14. Chou TC, Talalay (1983) Quantitative analysis of dose effect relationship: the combined effects of multiple drugs on enzyme inhibitors. In: Wever G (ed) Pergamon Press, New York, pp 27–55
15. deVere White RW, Deitch AD, Gumerlock PH, Shi S-B (1999) Use of a yeast assay to detect functional alterations in p53 in prostate cancer: a review and future directions. Prostate 41:134
16. Eastman A (1987) The formation, isolation, and characterization of DNA adducts produced by anticancer platinum complexes. Pharmacol Ther 34:155
17. Eastman A, Schulte N (1988) Enhanced DNA repair as a mechanism of resistance to cis-diamminedichloroplatinum(II). Biochemistry 27:4730
18. Edelman M, Gandara D (1996) Promising new agents in the treatment of lung cancer. Cancer Chemother Pharmacol 37:385
19. Fesquet D, Labbe JC, Derancourt J, Capony JP, Galas S, Girard F, Lorca T, Shuttleworth J, Doree M, Cavadore JC (1993) The MO15 gene encodes the catalytic subunit of a protein kinase that activates cdc2 and other cyclin-dependent kinases (CDKs) through phosphorylation of Thr161 and its homologues. EMBO J 8:3111
20. Fisher RP, Morgan DO (1994) A novel cyclin associates with MO15/CDK7 to form the CDK-activating kinase. Cell 78:713
21. Flaman JM, Frebourg T, Moreau V, Charbonnier F, Matyin C, Chappuis P, Sappino AP, Limacher JM, Bron L, Benhattar J, Tada M, van Meir EG, Estreicher A, Iggo RD (1995) A simple p53 functional assay for screening cell lines, blood, and tumors. Proc Natl Acad Sci USA 92:3963

22. Furnari B, Rhind N, Russell P (1997) Cdc25 mitotic inducer targeted by Chk1 DNA damage checkpoint kinase. Science 277:1495
23. Fuse E, Tanii H, Kurata N, Kobayashi H, Shimada Y, Tamura T, Sasaki Y, Tanigawara Y, Lush RD, Headlee D, Figg W, Arbuck SG, Senderowicz AM, Sausville EA, Akinaga S, Kuwabara T, Kobayashi S (1998) Unpredicted clinical pharmacology of UCN-01 caused by specific binding to human α1-acid glycoprotein. Cancer Res 58:3248
24. Fuse E, Hashimoto A, Sato N, Tanii H, Kuwabara T, Kobayashi S, Sugiyama Y (2000) Physiological modeling of altered pharmacokinetics of a novel anticancer drug, UCN-01 (7-hydroxystaurosporine), caused by slow dissociation of UCN-01 from human alpha1-acid glycoprotein. Pharm Res 17:553
25. Graves PR, Yu L, Schwartz JK, Gales J, Sausville EA, O'Connor PM, Piwnica-Worms H (2000) The Chk1 protein kinase and the Cdc25C regulatory pathways are targets of the anticancer agent UCN-01. J Biol Chem 275:5600
26. Harbour JW, Lai S-H, Whang-Peng J, Gazdar AF, Minna JD, Kaye FJ (1998) Abnormalities in structure and expression of the human retinoblastoma gene in SCLC. Science 241:353
27. Hirose Y, Berger MS, Pieper RO (2001) Abrogation of the Chk1-mediated G(2) checkpoint pathway potentiates temozolomide-induced toxicity in a p53-independent manner in human glioblastoma cells. Cancer Res 61:5843
28. Hsueh C-T, Wu Y-C, Schwartz GK (2001) UCN-01 suppresses E2F-1 mediated by ubiquitin-proteasome-dependent degradation. Clin Cancer Res 7:669
29. Husain A, Yan XJ, Rosales N, Aghajanian C, Schwartz GK, Spriggs DR (1997) UCN-01 in ovary cancer cells: effective as a single agent and in combination with cis-diamminedichloroplatinum(II) independent of p53 status. Clin Cancer Res 3:2089
30. Jiang H, Yang, L-Y (1999) Cell cycle checkpoint abrogator UCN-01 inhibits DNA repair: association with attenuation of the interaction of XPA and ERCC1 nucleotide excision repair. Cancer Res 59:4529
31. Jones CB, Clements MK, Wasi S, Daoud SS (2000) Enhancement of camptothecin-induced cytotoxicity with UCN-01 in breast cancer cells: abrogation of S/G2 arrest. Cancer Chemother Pharmacol 45:252
32. Kawakami K, Futami H, Takahara J, Yamaguchi K (1996) UCN-01 7-hydroxyl-staurosporine inhibits kinase activity of cyclin-dependent kinases and reduces phosphorylation of the retinoblastoma susceptibility gene product in A549 human lung cancer cell line. Biochem Biophys Res 219:778
33. Lau CC, Pardee AB (1982) Mechanism by which caffeine potentiates lethality of nitrogen mustard. Proc Natl Acad Sci USA 79:2942
34. Lee SI, Brown MK, Eastman A (1999) Comparison of the efficacy of 7-hydroxy staurosporine (UCN-01) and other staurosporine analogs to abrogate cisplatin-induced cell cycle arrest in human breast cancer cell lines. Biochemical Pharmacol 58:1713
35. Mack PC, Gandara DR, Bowen C, Edelman MJ, Paglieroni T, Schnier JB, Gelmann EP, Gumerlock PH (1999) RB status as a determinant of response to UCN-01 in non-small cell lung cancer. Clin Cancer Res 5:2596
36. Mitsudomi T, Steinberg SM, Nau MM, Carbone D, D'Amico D, Bodner S, Oie HK, Linoila RI, Mulshine JL, Minna JD, Gazdar AF (1992) p53 gene mutations in non-small-cell lung cancer cell lines and their correlation with the presence of ras mutations and clinical features. Oncogene 7:171
37. Mitsudomi T, Oyama T, Kusano T, Osaki T, Nakanishi R, Shirakusa T (1993) Mutations of the p53 gene as a predictor of poor prognosis with non-small-cell lung cancer. J Natl Cancer Inst 85:2018
38. Monks A, Harris ED, Vaigro-Wolff A, Hose CD, Connelly JW, Sausville EA (2000) UCN-01 enhances the in vitro toxicity of clinical agents in human tumor cell lines. Invest New Drugs 18; 95
39. Nurse P (1990) Universal control mechanism regulating onset of M-phase. Nature 344:503
40. Olivieri G, Micheli A (1983) Mitotic delay and repair in human lymphocytes. Mutat Res 122:65
41. Peng C-Y, Graves PR, Thoma RS, Wu Z, Shaw AS, Piwnica-Worms H (1997) Mitotic and G2 checkpoint control: regulation of 14-3-3 protein binding by phosphorylation of Cdc25C on serine-216. Science 277:1501
42. Poon RY, Yamashita K, Adamczewski JP, Hunt T, Shuttleworth J (1993) The cdc2-related protein p40MO15 is the catalytic subunit of a protein kinase that can activate p33cdk2 and p34cdc2. EMBO J 12:3123
43. Rhind N, Russell P (2000) Chk1 and Cds1: linchpins of the DNA damage and replication checkpoint pathways. J Cell Sci 113:3889
44. Roy KK, Sausville EA (2001) Early development of cyclin dependent kinase modulators. Curr Pharm Des 7:1669
45. Sampath D, Plunkett W (2001) Design of new anticancer therapies targeting cell cycle checkpoint pathways. Curr Opin Oncol 13:484
46. Sanchez Y, Wong C, Thoma RS, Richman R, Wu Z, Piwnica-Worms H, Elledge SJ (1997) Conservation of the Chk1 checkpoint pathway in mammals: linkage of DNA damage to cdk regulation through cdc25. Science 277:1497
47. Sausville EA, Arbuck SG, Messmann R, Headlee D, Bauer KS, Lush RM, Murgo A, Figg WD, Lahusen T, Jaken S, Jing X, Roberge M, Fuse E, Kuwabara T, Senderowicz AM (2001) Phase I trial of 72-hour continuous infusion UCN-01 in patients with refractory neoplasms. J Clin Oncol 19:2319
48. Senderowitcz AM (2002) The Cell Cycle as a target for cancer therapy: basic and clinical findings with small molecular inhibitors flavopiridol and UCN-01. Oncologist 7 [Suppl 3]:12
49. Seynaeve CM, Stetler-Stevenson M, Sebers S, Kaur G, Sausville EA, Worland PJ (1993) Cell cycle arrest and growth inhibition by the protein kinase antagonist UCN-01 in human breast carcinoma cells. Cancer Res 53:2081
50. Stewart N, Hicks GC, Paraskevas F, Mowat M (1995). Evidence for a second cell cycle block at G2/M by p53. Oncogene 10:109
51. Sugiyama K, Shimizu M, Akiyama T, Tamaoki T, Yamaguchi K, Eastman A, Akinaga S (2000) UCN-01 selectively enhances mitomycin C cytotoxicity in p53 defective cells which is mediated through S and/or G2 checkpoint abrogation. Int J Cancer 85:703
52. Takahashi I, Kobayashi E, Asano K, Yoshida M, Nakana H (1987) UCN-01, a selective inhibitor of protein kinase C from Streptomyces. J Antibiot 40:1782
53. Taylor WR, DePrimo SE, Agarwal A, Agarwal ML, Schonthal AH, Katula KS, Stark GR (1999) Mechanisms of G2 arrest in response to overexpression of p53. Mol Biol Cell 10:3607
54. Tsuchida E, Urano M (1997) The effects of UCN-01 (7-hydroxystaurosporine), a potent inhibitor of protein kinase C, on fractionated radiotherapy or daily chemotherapy of murine fibrosarcoma. Int J Radiat Oncol Biol Phys 39:1153
55. Wang Q, Worland P, Clark JL, Carlson BA, Sausville EA (1995) Apoptosis in 7-hydroxystaurosporine-treated T lymphoblasts correlates with activation of cyclin-dependent kinases 1 and 2. Cell Growth Differ 6:927
56. Wang Q, Fan S, Eastman A, Worland P, Sausville EA, O'Connor PM (1996) UCN-01: a potent abrogator of G2 checkpoint function in cancer cells with disrupted p53. J Natl Cancer Inst 88:956
57. Yamashita K, Yasuda H, Pines J, Yasumoto K, Nishitani H, Ohtsubo M, Hunter T, Sugimura T, Nishimoto T (1990) Okadaic acid, a potent inhibitor of type I and type 2A protein phosphatases, activates cdc2/H1 kinase and transiently induces a premature mitosis-like state in BHK21 cells. EMBO J 9:4331
58. Zwicker J, Lucibello FC, Wolfraim LA, Gross C, Truss M, Engeland K, Muller R (1995) Cell cycle regulation of the cyclin A, cdc25C and cdc2 genes is based on a common mechanism of transcriptional repression. EMBO J 14:4514